In Situ Calibration of Nucleoplasmic versus Cytoplasmic Ca^{2+} Concentration in Adult Cardiomyocytes

Senka Ljubojević,[†] Stefanie Walther,[†] Mojib Asgarzoei,[†] Simon Sedej,[†] Burkert Pieske,[†△*] and Jens Kockskämper[†‡△*]

[†]Division of Cardiology, Medical University of Graz, Graz, Austria; and [‡]Biochemical and Pharmacological Center Marburg, Institute of Pharmacology and Clinical Pharmacy, Philipps-University of Marburg, Marburg, Germany

ABSTRACT　Quantification of subcellularly resolved Ca^{2+} signals in cardiomyocytes is essential for understanding Ca^{2+} fluxes in excitation-contraction and excitation-transcription coupling. The properties of fluorescent indicators in intracellular compartments may differ, thus affecting the translation of Ca^{2+}-dependent fluorescence changes into [Ca^{2+}] changes. Therefore, we determined the in situ characteristics of a frequently used Ca^{2+} indicator, Fluo-4, and a ratiometric Ca^{2+} indicator, Asante Calcium Red, and evaluated their use for reporting and quantifying cytoplasmic and nucleoplasmic Ca^{2+} signals in isolated cardiomyocytes. Ca^{2+} calibration curves revealed significant differences in the apparent Ca^{2+} dissociation constants of Fluo-4 and Asante Calcium Red between cytoplasm and nucleoplasm. These parameters were used for transformation of fluorescence into nucleoplasmic and cytoplasmic [Ca^{2+}]. Resting and diastolic [Ca^{2+}] were always higher in the nucleoplasm. Systolic [Ca^{2+}] was usually higher in the cytoplasm, but some cells (15%) exhibited higher systolic [Ca^{2+}] in the nucleoplasm. Ca^{2+} store depletion or blockade of Ca^{2+} leak pathways eliminated the resting [Ca^{2+}] gradient between nucleoplasm and cytoplasm, whereas inhibition of inositol 1,4,5-trisphosphate receptors by 2-APB reversed it. The results suggest the presence of significant nucleoplasmic-to-cytoplasmic [Ca^{2+}] gradients in resting myocytes and during the cardiac cycle. Nucleoplasmic [Ca^{2+}] in cardiomyocytes may be regulated via two mechanisms: diffusion from the cytoplasm and active Ca^{2+} release via inositol 1,4,5-trisphosphate receptors from perinuclear Ca^{2+} stores.

INTRODUCTION

Quantification of subcellular Ca^{2+} concentration and fluxes is of crucial importance for understanding physiological and pathological processes in the heart (1,2). Nuclear Ca^{2+} regulates key cellular processes, including gene expression, apoptosis, assembly of the nuclear envelope, and nucleo-cytoplasmic transport (3–7). In cardiac myocytes, a transient rise in the cytoplasmic free Ca^{2+} concentration, [Ca^{2+}]$_{cyto}$, occurs during each heart beat. Each cytoplasmic [Ca^{2+}] transient (CaT) also elicits a nucleoplasmic CaT (8,9). However, it is not fully understood whether cytoplasmic CaTs transmit passively to the nucleus by Ca^{2+} diffusion through nuclear pore complexes, or whether nucleoplasmic [Ca^{2+}] ([Ca^{2+}]$_{nuc}$) can also be regulated actively, and, if so, by which mechanisms.

The notion that [Ca^{2+}]$_{nuc}$ does not just passively follow the [Ca^{2+}]$_{cyto}$ changes, but may instead be regulated actively and independently, is supported by evidence that the nuclear envelope expresses Ca^{2+}-regulating proteins, including the sarcoplasmic/endoplasmic reticulum Ca^{2+}-ATPase (SERCA), Ca^{2+} release channels, and Ca^{2+}-buffering proteins (10–13). Furthermore, it was previously shown that endothelin-1, via inositol 1,4,5-trisphosphate receptor (IP$_3$R)-mediated Ca^{2+} release from the nuclear envelope, may increase [Ca^{2+}]$_{nuc}$ independently from [Ca^{2+}]$_{cyto}$ (8). This process plays a key role in cardiac excitation-transcription coupling (14). It has also been implicated in the development of cardiac hypertrophy and the progression of heart failure (15–17), thus underlining the importance of elucidating the relationship between [Ca^{2+}]$_{nuc}$ and [Ca^{2+}]$_{cyto}$, and how Ca^{2+}-dependent signaling in the nucleus is regulated. However, this requires accurate measurements of [Ca^{2+}] in both the nucleoplasmic and cytoplasmic compartments.

The fluorescent indicators Fluo-3 and Fluo-4 are widely used to monitor [Ca^{2+}] in the cytoplasm and nucleoplasm of various cell types. Efforts to determine [Ca^{2+}]$_{nuc}$ versus [Ca^{2+}]$_{cyto}$ using these indicators, however, have been hindered by several technical difficulties and provided quite variable results. Some reports indicated that resting [Ca^{2+}]$_{nuc}$ is higher than [Ca^{2+}]$_{cyto}$ (18), but also the opposite was observed (19). In other cases, no difference between [Ca^{2+}]$_{nuc}$ and [Ca^{2+}]$_{cyto}$ was found (20), or it was attributed to artifacts (21). This discrepancy is in part caused by the fact that estimates of [Ca^{2+}]$_{nuc}$ changes are usually based on the assumption that Ca^{2+} indicators behave identically in different cellular compartments. This assumption, however, is not valid if the fluorescence properties of the dyes are altered differentially by the cytoplasmic and nucleoplasmic environment, as observed for Fluo-3 fluorescence in *Xenopus* oocyte nucleoplasmic and cytoplasmic homogenates (22). In situ studies with three different mouse cell lines loaded with either Fluo-3 or Fluo-4 yielded similar

results (23). A comparison of fluorescent Ca^{2+} indicator properties in HeLa cells further confirmed distinct characteristics of Fluo-3 and Fluo-4 in the cytoplasmic versus nucleoplasmic compartment (20). Further problems can arise from the sequestration of Ca^{2+} indicators into intracellular organelles (21,24). Indicators have also been reported to leak from the cytoplasm to the extracellular medium facilitated by sarcolemmal anion transporters (25,26).

Altogether, these observations indicate that without proper independent determination of the indicator properties in the nucleoplasm versus the cytoplasm, any quantitative analysis of $[Ca^{2+}]_{nuc}$ versus $[Ca^{2+}]_{cyto}$ is not reliable. Thus, to address the quantitative changes of $[Ca^{2+}]_{nuc}$ and $[Ca^{2+}]_{cyto}$, it will be necessary to transform raw fluorescence signals into calibrated $[Ca^{2+}]$, taking into account the effects of the different subcellular environments on the characteristics of the indicator. In cardiac myocytes, however, the Ca^{2+} binding affinities and fluorescent properties of Fluo indicators in different intracellular compartments have not yet been determined. In this study, first we determined the Ca^{2+}-dependent fluorescent properties of the frequently used Ca^{2+} indicator, Fluo-4, and of a new ratiometric Ca^{2+} indicator, Asante Calcium Red (ACaR), in the cytoplasm versus the nucleoplasm of cardiac myocytes by means of in situ calibration. Second, we used the results of the in situ calibration to quantify $[Ca^{2+}]_{cyto}$ and $[Ca^{2+}]_{nuc}$ signals under different physiological conditions in isolated cardiac myocytes. The results revealed that Fluo-4 and ACaR exhibit distinctively different fluorescent and Ca^{2+} binding properties between the cytoplasm and nucleoplasm of cardiomyocytes, and that there are significant nucleoplasmic-to-cytoplasmic $[Ca^{2+}]$ gradients in resting cardiomyocytes, that are dependent on intact 2-APB-sensitive Ca^{2+} stores.

MATERIALS AND METHODS

An expanded Materials and Methods section can be found in the Supporting Material.

Cell preparation and confocal Ca^{2+} imaging

The experimental procedures used to isolate cardiomyocytes from rat and mouse hearts were approved by the local Animal Care and Use Committees according to criteria outlined in the *Guide for the Care and Use of Laboratory Animals* prepared by the U.S. National Academy of Sciences (National Institutes of Health publication No. 85-23, revised 1996). Isolated cardiomyocytes were loaded with Fluo-4 (Molecular Probes, Eugene, OR) by 30-min incubation in normal Tyrode's solution (NT) containing 8 μM of the acetoxymethylester (AM) of the dye (in 20% (w/v) Pluronic-127/dimethyl sulfoxide (DMSO); Molecular Probes). A further 30 min were allowed for deesterification. When ACaR was used, the myocytes were incubated with 10 μM ACaR AM (TEFLabs, Austin, TX) for 90 min, and 45 min were allowed for deesterification. All experiments were conducted at room temperature (22–24°C).

Fast, two-dimensional (2D) confocal $[Ca^{2+}]$ imaging was performed as described previously (27) with the use of a confocal imaging setup (VisiTech International, Sunderland, UK) based on a Nipkow disc. Alternatively,

a Zeiss LSM 510 Meta confocal microscope (Carl Zeiss, Jena, Germany) was used. For Fluo-4, the excitation and emission wavelengths were 488 nm and >515 nm, respectively. For ACaR, excitation occurred at 488 nm and emission was collected at >650 nm (F$_1$) and at 475–525 nm (F$_2$). The z-axis resolution of the confocal images was ~0.9–1.4 μm. The height of the nuclei amounted to 5–7 μm. For recording of $[Ca^{2+}]_{nuc}$, the confocal plane was set to the middle (z axis) of the nuclei to ensure that only fluorescence originating from the nucleoplasm would be collected.

In situ calibration of Fluo-4 and ACaR fluorescence

Calibration solutions were made according to the procedure described by Bers (28) and McGuigan et al. (29). In brief, we calculated the total $[Ca^{2+}]$ required to obtain the desired free $[Ca^{2+}]$ in the presence of 1mM EGTA using the MaxChelator program (30) (http://www.stanford.edu/~cpatton/maxc.html). Two solutions (EGTA and CaEGTA) were prepared. The EGTA solution contained (mM) 130 NaCl, 5.4 KCl, 0.5 MgCl$_2$, 1 EGTA, 15 BDM (2,3 butanedione monoxime), 25 Hepes, 0.01 A23187, 1.8 2-deoxy-D-glucose, 0.01 rotenone, 0.005 CPA, pH 7.4. The CaEGTA solution was the same as the EGTA solution except that it also contained 2 mM CaCl$_2$. Known quantities of EGTA and CaEGTA solutions were mixed to obtain calibration solutions with free $[Ca^{2+}]$ of 0 nM, 50 nM, 250 nM, 750 nM, 1500 nM, 3000 nM, and 1 mM. The free $[Ca^{2+}]$ was confirmed with a Ca^{2+}-sensitive electrode (Orion 97-20 ionplus; Thermo Electron, Beverly, MA). Calibration solutions also contained the Ca^{2+} ionophore A23187, metabolic inhibitors (2-deoxy-D-glucose, 1.8 mM; rotenone, 10 μM) and cyclopiazonic acid (CPA, 5 μM), a SERCA inhibitor, to block active Ca^{2+} transport systems and allow equilibration of $[Ca^{2+}]$ between the extracellular medium and the cell interior (20). Finally, the calibration solutions contained butanedione monoxime (BDM) to prevent contracture of the myocytes at high $[Ca^{2+}]$. Cells were equilibrated in each calibration solution for 8 min. During this period, fluorescence was averaged over 1-s intervals every 2 min. Minimal Fluo-4 or ACaR fluorescence (F$_{min}$) was measured during exposure to Ca^{2+}-free calibration solution and maximal Fluo-4 or ACaR fluorescence (F$_{max}$) during exposure to a calibration solution containing a saturating free $[Ca^{2+}]$ of 1 mM.

Drugs and solutions

We obtained 2-APB, A23187, CPA, and rotenone from Calbiochem (Darmstadt, Germany). All other chemicals were purchased from Sigma-Aldrich Chemie GmbH (Steinheim, Germany). The drugs were dissolved in DMSO as concentrated stock solutions and diluted at least 1000-fold into the medium. This yielded a final DMSO concentration of $\leq 0.1\%$, which on its own showed no effect on myocyte morphology and contractile function.

Statistics

The data are presented as the mean $\pm$ standard error (SE). Differences between data sets were evaluated by Student's *t*-test or analysis of variance, and were considered significant when $p < 0.05$.

RESULTS

In situ calibration of Fluo-4 fluorescence in cardiac myocytes

Mouse ventricular myocytes and rat atrial and ventricular myocytes were loaded with the fluorescent Ca^{2+} indicator Fluo-4 by incubation with the acetoxymethyl ester form of the dye. Because Fluo-4 fluorescence changes do not

directly report changes in the free $[Ca^{2+}]$, the fluorescence signals had to be transformed into calibrated $[Ca^{2+}]$. The most commonly used approach to transform Fluo-4 fluorescence into free $[Ca^{2+}]$ is to apply the equation first formulated by Grynkiewicz and colleagues (31). For nonratiometric dyes, the formula is as follows:

$$[Ca^{2+}] = K_d (F - F_{min})/(F_{max} - F) \quad (1)$$

where K_d is the apparent Ca^{2+} dissociation constant of the indicator; F_{min} and F_{max} are the fluorescence intensities at zero and saturating $[Ca^{2+}]$, respectively; and F is the fluorescence intensity at any given time. Obviously, the derivation of $[Ca^{2+}]$ depends on two parameters, F_{min} and F_{max}, which have to be determined independently for each cell measured. As we sought to define the equation in a way that includes only the indicator's properties that can be predetermined, we transformed the original formula using the equation for the resting $[Ca^{2+}]$, $[Ca^{2+}]_{rest}$:

$$[Ca^{2+}]_{rest} = K_d (F_{rest} - F_{min})/(F_{max} - F_{rest}) \quad (2)$$

and the dynamic range of the indicator, R_f:

$$R_f = F_{max}/F_{min} \quad (3)$$

We eliminated the parameters F_{min} and F_{max} from Eq. 1 by substituting them with Eqs. 2 and 3, and thus obtained the final formula for transforming the fluorescence signals into absolute $[Ca^{2+}]$:

$$[Ca^{2+}] = K_d (R(K_d + R_f [Ca^{2+}]_{rest}) - (K_d + [Ca^{2+}]_{rest}))/(R_f (K_d + [Ca^{2+}]_{rest}) - R(K_d + R_f [Ca^{2+}]_{rest})) \quad (4)$$

where R is the normalized fluorescence signal, F/F_{rest}.

The key parameters in Eq. 4 are K_d, $[Ca^{2+}]_{rest}$, and R_f. Therefore, fluorescent signals from nucleoplasmic and cytoplasmic compartments with seven different $[Ca^{2+}]$ values ranging from 0 nM to 1 mM were obtained from mouse ventricular ($n = 15$) and rat atrial ($n = 8$) and ventricular ($n = 15$) cardiac myocytes (Fig. 1). The calibration solutions contained a Ca^{2+} ionophore, metabolic inhibitors, an inhibitor of SERCA, and BDM. This allowed rapid and complete equilibration of $[Ca^{2+}]$ between the extracellular solution and the cell interior, and prevented any active Ca^{2+} transport as well as movement and contracture of the cells at higher $[Ca^{2+}]$. Fig. 1 A shows original images of a mouse cardiac myocyte obtained with selected $[Ca^{2+}]$
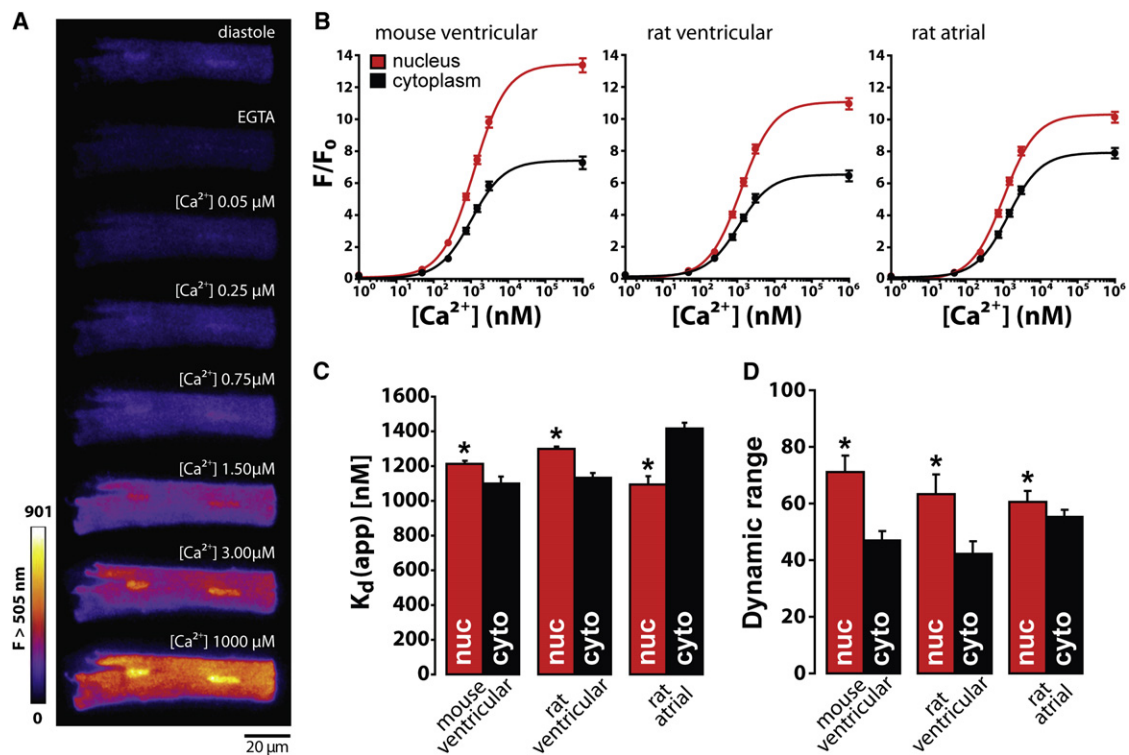

FIGURE 1 In situ calibration of fluorescent Ca^{2+} indicator Fluo-4 in the nucleus versus the cytoplasm of mouse and rat cardiac myocytes. (A) Original 2D images of Fluo-4 fluorescence of a mouse ventricular myocyte at various $[Ca^{2+}]$ values during the calibration protocol. (B) Concentration response curves with seven different $[Ca^{2+}]$ values, illustrating the in situ Ca^{2+}-dependent fluorescence of Fluo-4 in the nucleus (red) versus the cytoplasm (black) of mouse ventricular, rat atrial, and rat ventricular myocytes. (C) Apparent dissociation constants for Ca^{2+} binding ($K_{d(app)}$) and (D) dynamic range of Fluo-4 fluorescence in the nucleus (red) versus the cytoplasm (black). Data in B–D were obtained from a total of 15 mouse ventricular, eight rat atrial, and 15 rat ventricular myocytes. Asterisks indicate $p < 0.05$ versus cytoplasm.

solutions during the calibration protocol. The Fluo-4 fluorescence from the nucleus was higher than that from the surrounding cytoplasm at each [Ca^{2+}] used, and this was true for all cell types studied. We plotted the nucleoplasmic and cytoplasmic Fluo-4 fluorescence versus [Ca^{2+}] (Fig. 1 B) and then fitted the concentration-response curves using the Hill equation:

$$F = \left\{ (F_{max} - F_{min}) / \left(1 + \left(K_d / [Ca^{2+}] \right)^n \right) \right\} + F_{min} \quad (5)$$

This allowed us to determine the in situ Ca^{2+} dissociation constant (K_d) and the Hill coefficient (n). We also assessed photobleaching of the Ca^{2+} indicator Fluo-4 over the course of the protocol and found it to be negligible (not shown). The obtained calibration curves were used to calculate the apparent K_d and the dynamic range, R_f. Fluo-4 showed significantly different Ca^{2+} binding affinities between the nucleoplasmic and cytoplasmic compartments in all cell types studied (Fig. 1 C). Higher apparent K_d-values were found in the nucleoplasm of mouse and rat ventricular myocytes, but not in rat atrial myocytes, where the apparent K_d in the nucleoplasm was lower than in the cytoplasm. Furthermore, significantly higher values for R_f were found in nucleoplasmic as compared with the cytoplasmic compartments of all three cell types studied (Fig. 1 D). Within a given cell type, the results were uniform and independent of dye loading and gain settings. Once they were determined, the average values for $K_{d,app}$, [Ca^{2+}]$_{rest}$, and R_f were used in Eq. 4 for further transformation of the fluorescence signals. For cells in which all calibration parameters had been measured, we compared the [Ca^{2+}] values calculated by Eqs. 1 and 4. We observed no significant difference for electrically stimulated CaTs calculated by these two methods. This confirms that the use of $K_{d,app}$, R_f, and [Ca^{2+}]$_{rest}$ (as determined with the calibration protocol) in combination with Eq. 4 is well suited for calculating [Ca^{2+}]$_{cyto}$ and [Ca^{2+}]$_{nuc}$ in the same type of myocytes, isolated under the same experimental conditions, in which no calibration has been conducted.

Cardiomyocytes loaded with Fluo-4 generally displayed uniform cellular fluorescence patterns without obvious accumulation in subcellular organelles (except for the nuclei). The nuclei of cells loaded with Fluo-4 possessed a higher fluorescence than that of the surrounding cytoplasm. Experiments in which the compartmentalization of Fluo-4 was evaluated revealed that >90% of the dye was distributed in the cytoplasm and nucleoplasm (Fig. S2).

In situ calibration of ACaR fluorescence in cardiac myocytes

To validate the results obtained with the nonratiometric Ca^{2+} indicator Fluo-4, we also conducted in situ calibration experiments using the ratiometric Ca^{2+} indicator ACaR. Fig. 2 A illustrates original images of a ventricular myocyte

obtained before (diastole) and during the calibration procedure at various [Ca^{2+}] values. Fluorescence emissions at >650 nm (F$_1$, *left*) and 475–525 nm (F$_2$, *middle*), as well as the ratio F$_1$/F$_2$ (*right*), are shown. With increasing [Ca^{2+}], F$_1$ increased, whereas F$_2$ decreased, as expected from the emission spectra of ACaR. Consequently, the ratio F$_1$/F$_2$ also increased with increasing [Ca^{2+}]. In similarity to Fluo-4, ACaR exhibited higher fluorescence in the nucleoplasm than in the cytoplasm.

We plotted the ratio F$_1$/F$_2$ as a function of [Ca^{2+}] (Fig. 2 B) and used the Hill equation to fit and obtain the $K_{d,app}$ for Ca^{2+} binding. In a total of 15 ventricular myocytes, $K_{d,app}$ amounted to 2183 $\pm$ 55 nM in the nucleoplasm, and 1336 $\pm$ 38 nM in the cytoplasm (Fig. 2 C). Thus, similarly to Fluo-4, ACaR displayed different $K_{d,app}$-values for Ca^{2+} binding in the nucleoplasm versus cytoplasm.

Having obtained the in situ $K_{d,app}$ for Ca^{2+} binding, we used the Grynkiewicz formula for ratiometric dyes to calculate [Ca^{2+}]$_{cyto}$ and [Ca^{2+}]$_{nuc}$:

$$[Ca^{2+}] = K_d \, \beta \, (R - R_{min}) / (R_{max} - R) \quad (6)$$

where $R = F_1/F_2$, $R_{min} = F_1/F_2$ in the absence of Ca^{2+}, $R_{max} = F_1/F_2$ in the presence of saturating [Ca^{2+}], and β = the proportionality factor determined by the ratio of the F$_2$ intensities of free and Ca^{2+}-bound dye, respectively (31).

Quantification and characterization of cytoplasmic and nucleoplasmic CaTs in electrically stimulated cardiac myocytes

The established in situ calibration curves were used to transform the raw fluorescence signal during an electrically stimulated CaT into [Ca^{2+}]$_{nuc}$ and [Ca^{2+}]$_{cyto}$. Fig. 3 A shows original traces from the nucleus and cytoplasm of two mouse cardiac myocytes. The traces on the left show a typical example of the CaTs observed in most of the cells studied (85%): diastolic [Ca^{2+}]$_{nuc}$ was higher (in all cells studied), whereas systolic [Ca^{2+}]$_{nuc}$ was lower than in the cytoplasm. Of interest, however, some of the cells (15%) showed higher systolic [Ca^{2+}] in the nucleus than in the cytoplasm (*traces on the right*). On average, there was a significant difference in diastolic and systolic [Ca^{2+}] between the cytoplasmic and nucleoplasmic compartments in all three types of cardiac myocytes: diastolic [Ca^{2+}] was higher, whereas systolic [Ca^{2+}] was lower in the nucleus (Fig. 3 B). The kinetics of the CaTs were significantly slower in the nucleoplasm than in the cytoplasm, and this was true for all myocytes studied (n = 70; Fig. 3 C). There was a weak but significant correlation between nucleoplasmic and cytoplasmic diastolic [Ca^{2+}], and a much higher correlation between nucleoplasmic and cytoplasmic systolic [Ca^{2+}] (Fig. S2).

Measurements with the ratiometric indicator ACaR (n = 15) yielded almost identical results (Fig. 3, A–C, right). Two
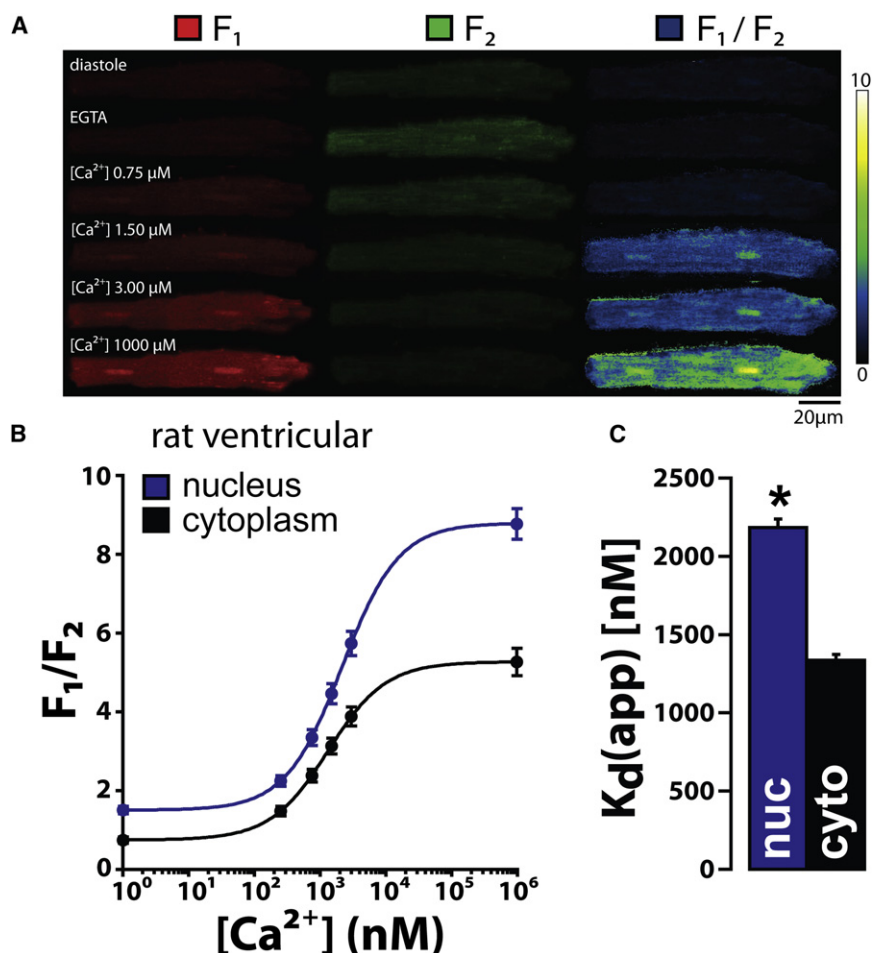
FIGURE 2   In situ calibration of the ratiometric Ca^{2+} indicator ACaR in the nucleus versus cytoplasm of rat ventricular myocytes. (*A*) Original 2D images of ACaR fluorescence at >650 nm (F1, *left*) and 475–525 nm (F2, *middle*), as well as the ratio F1/F2 (*right*), of a rat ventricular myocyte at various $[Ca^{2+}]$ during the calibration protocol. (*B*) Concentration response curves of the ratio F1/F2 as a function of $[Ca^{2+}]$ in the nucleus (*blue*) versus the cytoplasm (*black*) of rat ventricular myocytes. (*C*) $K_{d(app)}$ for Ca^{2+} binding in the nucleus (*blue*) versus the cytoplasm (*black*). Data from 15 rat ventricular myocytes. Asterisk indicates $p < 0.05$ versus cytoplasm.

out of 15 cells (13%) showed higher systolic $[Ca^{2+}]$ in the nucleoplasm versus cytoplasm and all cells showed higher diastolic $[Ca^{2+}]$ in the nucleoplasm.

Taken together, these data imply the following: 1), diastolic and systolic $[Ca^{2+}]$ levels in the nucleus depend to some extent on $[Ca^{2+}]$ levels in the cytoplasm; 2), diastolic $[Ca^{2+}]$ in the nucleus is always higher than diastolic $[Ca^{2+}]$ in the cytoplasm, suggesting active release of Ca^{2+} into and/ or slowed removal of Ca^{2+} from the nucleus; and 3), there may be both a passive and an active component of Ca^{2+} increase during the spread of the cytoplasmic CaT into the nucleus.

Resting $[Ca^{2+}]_{cyto}$ and $[Ca^{2+}]_{nuc}$ before and after depletion of intracellular Ca^{2+} stores

To elucidate the reason for the higher diastolic $[Ca^{2+}]$ in the nucleus, we investigated in more detail the resting $[Ca^{2+}]$ values in the two compartments. Fig. 4 *A* shows that even in resting myocytes, the gradient between nucleus and cytoplasm persisted, i.e., $[Ca^{2+}]_{nuc}$ was still significantly higher than $[Ca^{2+}]_{cyto}$ in all cell types studied, irrespective of the Ca^{2+} indicator used (Fluo-4 or ACaR). This indicates that

the difference in diastolic $[Ca^{2+}]$ between the two compartments during electrical stimulation (Fig. 3) cannot be explained entirely by differences in the kinetics of the CaTs (see also below). We hypothesized that the difference in resting $[Ca^{2+}]$ was caused by a Ca^{2+} release from the perinuclear calcium stores into the nucleoplasm. If this nucleoplasmic Ca^{2+} leak was higher than the cytoplasmic Ca^{2+} leak, i.e., Ca^{2+} released from the sarcoplasmic reticulum (SR) into the cytoplasm, this could explain the diastolic $[Ca^{2+}]$ gradient between the nucleus and the cytoplasm. To test this hypothesis, we depleted the intracellular Ca^{2+} stores using CPA and Ca^{2+}-free solution. Fig. 4 *B* illustrates an original recording from a mouse ventricular myocyte. In the resting cell in the presence of NT, $[Ca^{2+}]_{nuc}$ was higher than $[Ca^{2+}]_{cyto}$. Shortly after the addition of CPA in Ca^{2+}-free solution, $[Ca^{2+}]$ rose in both the nucleus and the cytoplasm, presumably because of an imbalance between uptake and release from the internal stores, with uptake being blocked by CPA. $[Ca^{2+}]_{nuc}$ still exceeded $[Ca^{2+}]_{cyto}$ during this phase. The Ca^{2+} elevation was transient, though, because plasma membrane Ca^{2+} transport systems were still functioning and capable of extruding the ions out of the cell. Finally, $[Ca^{2+}]_{nuc}$ and $[Ca^{2+}]_{cyto}$ returned close to the
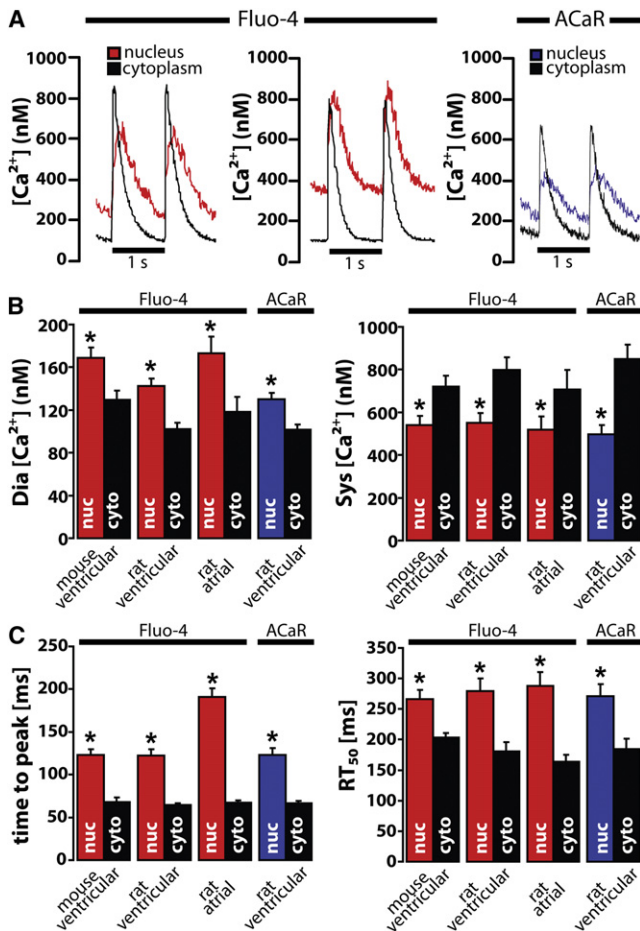
FIGURE 3 Quantification and characterization of cytoplasmic and nucleoplasmic CaTs in electrically stimulated cardiac myocytes. (A) Original recordings of electrically stimulated CaTs in the nucleus versus cytoplasm (*black*) of three ventricular myocytes. Traces on the left and right show typical examples for most of the cells studied (85%): diastolic nucleoplasmic [Ca^{2+}] was higher, whereas systolic nucleoplasmic [Ca^{2+}] was lower than in the cytoplasm. A minority of cells (15%) showed higher systolic [Ca^{2+}] in the nucleus as compared with the cytoplasm (*middle traces*). (B) Diastolic and systolic [Ca^{2+}] and (C) kinetic parameters (time to peak (*left*) and RT$_{50}$ (*right*)) of the CaTs. Data in B and C were obtained from a total of 15 mouse ventricular, eight rat atrial, and 15 rat ventricular myocytes for Fluo-4, and 15 rat ventricular myocytes for ACaR. Asterisks indicate $p < 0.05$ versus cytoplasm.

resting values. Of importance, however, the gradient between the nucleus and the cytoplasm had vanished. Fig. 4 C shows that after the Ca^{2+} store was depleted, [Ca^{2+}]$_{nuc}$ and [Ca^{2+}]$_{cyto}$ were essentially identical ($n = 12$). This indicates that the nucleoplasmic-to-cytoplasmic [Ca^{2+}] gradient in resting myocytes depends on intact intracellular Ca^{2+} stores.

Effects of 2-APB and tetracaine on the nucleoplasmic-to-cytoplasmic [Ca^{2+}] gradient

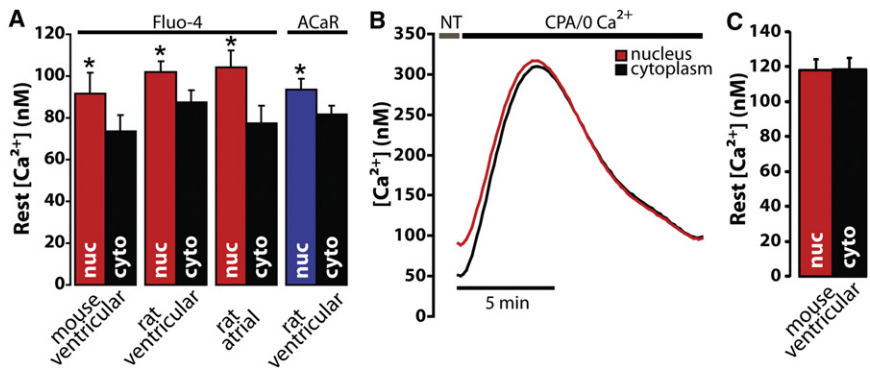We hypothesized that a tonic Ca^{2+} leak from perinuclear Ca^{2+} stores caused the nucleoplasmic-to-cytoplasmic [Ca^{2+}]

gradient observed in resting myocytes. To identify the Ca^{2+} release channel(s) involved, we conducted experiments with 2-APB (3 μM), a blocker of IP$_3$Rs, and tetracaine (1 mM), a blocker of ryanodine receptors (RyR2). Fig. 5 A shows an original recording from a ventricular myocyte. Average results are presented in Fig. 5 C. In NT, [Ca^{2+}]$_{nuc}$ was higher than [Ca^{2+}]$_{cyto}$. Exposure of the cell to 2-APB decreased [Ca^{2+}]$_{nuc}$, whereas [Ca^{2+}]$_{cyto}$ remained almost unchanged. Thus, the nucleoplasmic-to-cytoplasmic [Ca^{2+}] gradient was completely reversed. Additional application of tetracaine reduced predominantly [Ca^{2+}]$_{cyto}$. In the presence of both 2-APB and tetracaine, there was no nucleoplasmic-to-cytoplasmic [Ca^{2+}] gradient. When tetracaine was applied first (Fig. 5, B and D), there was a decrease in both nucleo- and cytoplasmic [Ca^{2+}]. Of importance, however, [Ca^{2+}]$_{nuc}$ remained higher than [Ca^{2+}]$_{cyto}$. Additional application of 2-APB caused a selective decrease in [Ca^{2+}]$_{nuc}$. Again, in the presence of both inhibitors, there was no nucleoplasmic-to-cytoplasmic [Ca^{2+}] gradient. These results show that the nucleoplasmic-to-cytoplasmic [Ca^{2+}] gradient depends on a Ca^{2+} leak from intracellular Ca^{2+} stores. The fact that 2-APB caused selective decreases of [Ca^{2+}]$_{nuc}$ and could even reverse the gradient suggests that there is a tonic IP$_3$R-mediated Ca^{2+} leak from perinuclear Ca^{2+} stores that is responsible for the higher [Ca^{2+}]$_{nuc}$ in resting myocytes.

When electrically stimulated ventricular myocytes were exposed to 2-APB (3 μM), we observed a selective decrease of diastolic nucleoplasmic [Ca^{2+}] (Fig. 5, E and F). Systolic nucleoplasmic [Ca^{2+}] and cytoplasmic [Ca^{2+}] in both diastole and systole remained unaffected. Thus, consistent with the results obtained in resting myocytes, an IP$_3$R-mediated Ca^{2+} leak/release from perinuclear Ca^{2+} stores appeared to contribute to nucleoplasmic Ca^{2+} regulation, particularly in diastole, whereas systolic [Ca^{2+}] in the nucleoplasm seemed to be governed predominantly by the cytoplasmic [Ca^{2+}] increase and diffusion of Ca^{2+} through nuclear pores into the nucleoplasm (see also Fig. S3).

Stimulation frequency-dependent changes in [Ca^{2+}]$_{nuc}$ versus [Ca^{2+}]$_{cyto}$

Heart rate is an important determinant of cardiac function. In cardiac myocytes, increases in stimulation frequency cause increases in diastolic and systolic [Ca^{2+}]. Because of the markedly slower kinetics of nucleoplasmic CaTs as compared with cytoplasmic CaTs (Fig. 3), we hypothesized that an increase in stimulation frequency would affect [Ca^{2+}]$_{nuc}$ and [Ca^{2+}]$_{cyto}$, and in particular the diastolic [Ca^{2+}], differentially. Fig. 6 A shows an original recording from a mouse ventricular myocyte. The stimulation frequency was gradually increased from 0.5 Hz to 4 Hz. Both diastolic and systolic [Ca^{2+}] values in the nucleus and cytoplasm rose with the increase in frequency. However, the increase was most pronounced for diastolic [Ca^{2+}] in the nucleus. Fig. 6 B shows average data obtained from

FIGURE 4 Resting cytoplasmic and nucleoplasmic [Ca^{2+}] before and after depletion of intracellular Ca^{2+} stores. (A) Calibrated resting [Ca^{2+}] in mouse ventricular (n = 15), rat atrial (n = 8), and rat ventricular (n = 15 for both Fluo-4 and ACaR) myocytes show significantly higher values in the nucleus than in the cytoplasm. Asterisks indicate p < 0.05 versus cytoplasm. (B) Original recording of nucleoplasmic and cytoplasmic (black) [Ca^{2+}] of a mouse ventricular myocyte before (NT) and during the depletion of intracellular Ca^{2+} stores by means of CPA and zero Ca^{2+} solution. Note that the difference between nucleoplasmic and cytoplasmic [Ca^{2+}] evident in NT vanishes during depletion of the Ca^{2+} stores. (C) Resting [Ca^{2+}] in a total of 12 mouse ventricular myocytes after depletion of intracellular Ca^{2+} stores. Resting [Ca^{2+}]$_{nuc}$ and [Ca^{2+}]$_{cyto}$ were essentially identical under these conditions, indicating that the nucleoplasmic-to-cytoplasmic [Ca^{2+}] gradient observed in NT depended on the intracellular Ca^{2+} store content.

20 myocytes, which confirm this observation. Systolic [Ca^{2+}] in the cytoplasm and nucleoplasm increased in parallel, whereas the diastolic [Ca^{2+}] increase in the nucleus by far exceeded that in the cytoplasm. These results show that because of the slower CaT kinetics in the nucleus, an increase in stimulation frequency is sufficient for differential regulation of diastolic [Ca^{2+}] in the nucleus versus the cytoplasm.
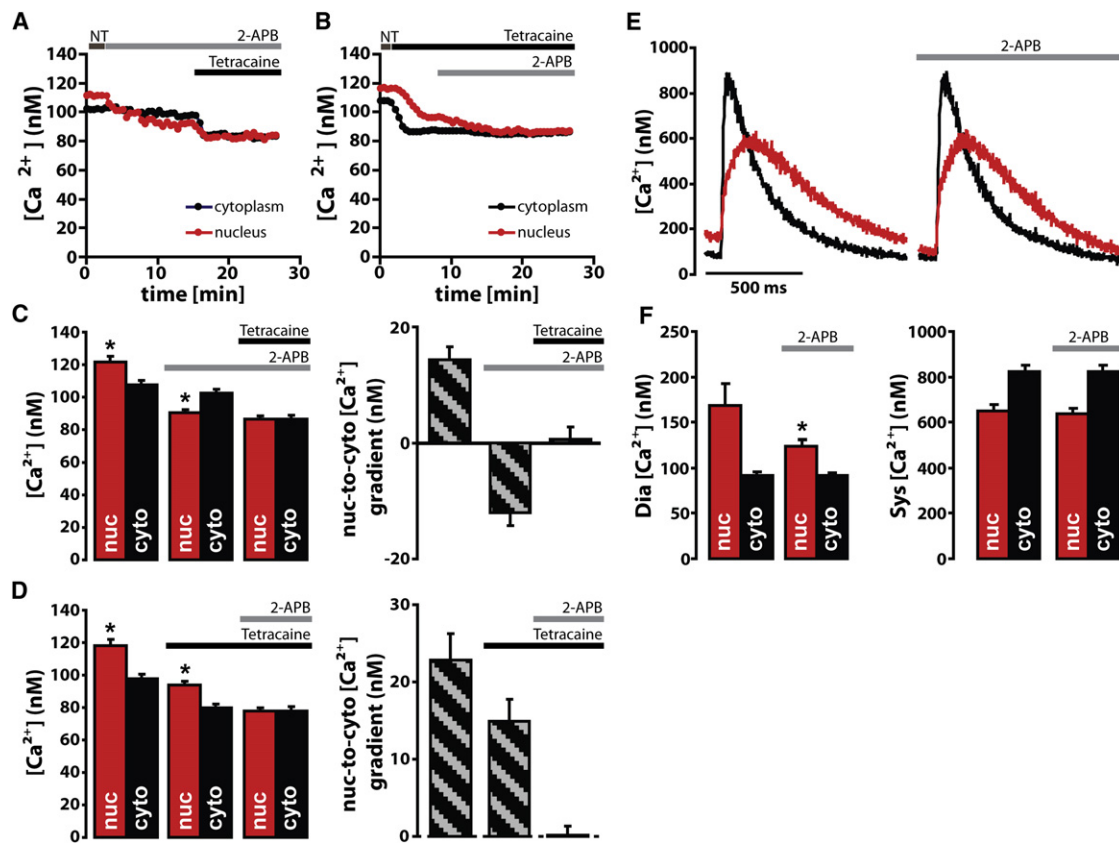

FIGURE 5 Effects of 2-APB and tetracaine on the nucleoplasmic-to-cytoplasmic [Ca^{2+}] gradient. (A and B) Original recordings of resting [Ca^{2+}]$_{nuc}$ versus [Ca^{2+}]$_{cyto}$ (black) of two rat ventricular myocytes before (NT) and after application of 2-APB and tetracaine. (C and D) Average values of resting [Ca^{2+}]$_{nuc}$ versus [Ca^{2+}]$_{cyto}$ (black) and of the nucleoplasmic-to-cytoplasmic [Ca^{2+}] gradient of rat ventricular myocytes before (NT) and after application of 2-APB and tetracaine. Data were obtained from a total of 10 rat ventricular myocytes for each series. Asterisks indicate p < 0.05 versus cytoplasm. (E) Original recordings of [Ca^{2+}]$_{nuc}$ versus [Ca^{2+}]$_{cyto}$ (black) transients in an electrically stimulated rat ventricular myocyte before and after application of 2-APB. (F) Average values of diastolic and systolic [Ca^{2+}]$_{nuc}$ versus [Ca^{2+}]$_{cyto}$ (black) from a total of 15 electrically stimulated rat ventricular myocytes before and after application of 2-APB. Asterisk indicates p < 0.05 versus [Ca^{2+}]$_{nuc}$ under control conditions.
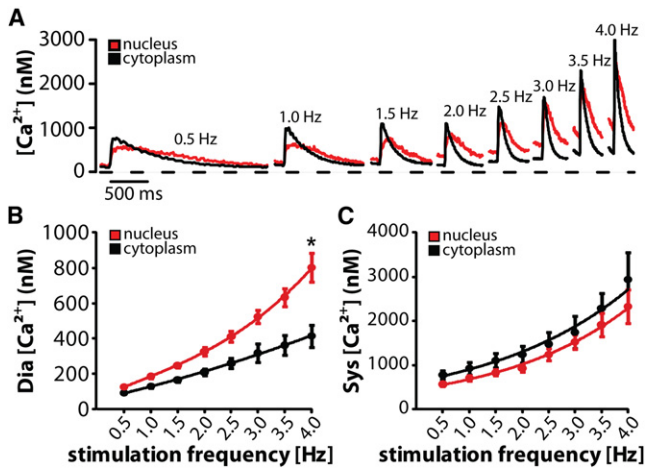
FIGURE 6 Frequency-dependent increases in diastolic and systolic [Ca^{2+}] in the nucleus versus the cytoplasm. (*A*) Original recording of electrically stimulated CaTs in the nucleus versus the cytoplasm (*black*) of a mouse ventricular myocyte during gradual increases of stimulation frequency from 0.5 Hz to 4 Hz. Average values of diastolic and systolic [Ca^{2+}] from a total of 20 mouse ventricular myocytes are shown in *B* and *C*, respectively. The frequency-dependent increase in diastolic [Ca^{2+}] in the nucleus was significantly larger ($p < 0.05$) than in the cytoplasm.

DISCUSSION

In situ calibration of Fluo-4 and ACaR fluorescence

The in situ calibration procedure described here provides a new (to our knowledge) means of quantifying [Ca^{2+}]$_{nuc}$ versus [Ca^{2+}]$_{cyto}$ changes in cardiomyocytes for both Fluo-4 and ACaR.

Previous studies showed that the fluorescent properties of the Ca^{2+} indicator Fluo-4 are altered by the nuclear environment of various cell types (20,23). Therefore, we evaluated two sets of Fluo-4 parameters, cytosolic and nucleoplasmic, in mouse and rat cardiac myocytes. Our results for the mouse and rat ventricular cardiac myocytes are in good agreement with previous findings in HeLa cells, where the K$_{d,app}$ amounted to ~1000 nM in the cytoplasm (versus ~1100 nM in our study) and to ~1260 nM in the nucleoplasm (versus ~1200–1300 nM in our study) (20). However, the opposite was observed in rat atrial myocytes, where the K$_{d,app}$ was higher in the cytoplasm (~1400 nM) than in the nucleoplasm (~1100 nM). The reason for this difference between atrial and ventricular myocytes is unknown at present, but it is probably related to the fact that the K$_{d,app}$ for Ca^{2+} binding of the fluorescent probe can be drastically affected by environmental conditions. This implies that there may be substantial differences between atrial and ventricular myocytes in terms of the nuclear environment, at least with respect to the physicochemical properties of Fluo-4.

Our calibration method also relies on estimates of the dynamic range, R$_f$, and [Ca^{2+}]$_{rest}$. The dynamic range was previously described as a property of the indicator that

does not need to be determined for every experiment (32). However, previously obtained values for the dynamic range of Fluo-4 varied. Thomas and colleagues (20) found it to be 6 and 15 for the cytoplasm and nucleoplasm of HeLa cells, respectively, whereas values of 85–100 have also been observed (32). In the context of this study—more important than the exact value of R$_f$, which can vary depending on the cell type and experimental conditions—it is to note that the results were uniform within a given cell type, and were independent of dye loading and gain settings. This justifies the use of the dynamic range as a parameter for transforming fluorescence into calibrated [Ca^{2+}]. The dynamic range in the nucleoplasm was consistently higher than in the cytoplasm, and this was true for all types of cardiac myocytes studied. This is in perfect agreement with previous studies on noncardiac myocytes (20,23). Cellular resting [Ca^{2+}] may also vary (20–200 nM) depending on the state and type of the cell (33). In cardiac myocytes, it is usually assumed to be in the range of ≤100 nM. Here, we found that [Ca^{2+}]$_{rest}$-values varied only in a narrow range in each cell type studied, as well as between cell types. The [Ca^{2+}]$_{rest}$-values amounted to ~80 nM in the cytoplasm and ~100 nM in the nucleoplasm. This suggests that their mean is a valid parameter for calibration.

We further compared [Ca^{2+}] values obtained using different forms of the Grynkiewicz equation. No significant difference was observed with either Eq. 1 or Eq. 4. Conversely, results calculated from [Ca^{2+}]$_{rest}$, assuming that F$_{rest}$ ≈ 0 (34):

$$\left[\text{Ca}^{2+}\right] = \text{K}_d \, \text{R} / \left(\text{K}_d / \left[\text{Ca}^{2+}\right]_{rest} - \text{R} + 1\right) \tag{7}$$

yielded significantly lower values. This important difference reflects the fact that cellular [Ca^{2+}]$_{rest}$ levels are not negligible for indicators with very bright fluorescence, like Fluo-4, which typically makes F$_{rest}$ considerably larger than F$_{min}$.

The advantage of this method is that all parameters that are necessary for the transformation of Fluo-4 fluorescence signals into calibrated [Ca^{2+}] can be predetermined, which makes this process very convenient for practical use with mouse and rat cardiac myocytes.

We also determined for the first time in cardiomyocytes (to our knowledge) the in situ properties of the ratiometric Ca^{2+} dye ACaR. In similarity to Fluo-4, ACaR exhibited different fluorescent properties in the nucleoplasm versus the cytoplasm, with larger Ca^{2+}-dependent fluorescence changes and a higher K$_{d,app}$ in the nucleoplasm. Also, similarly to most fluorescent Ca^{2+} dyes tested so far, the in situ determination of K$_{d,app}$ revealed considerably higher values (~2200 nM in the nucleoplasm and ~1340 nM in the cytoplasm) than in vitro (according to the manufacturer's information: K$_d$ ~300–400 nM). Ca^{2+}-dependent fluorescence changes, as well as electrically stimulated [Ca^{2+}] transients, could be easily detected at both wavelengths during calibration. Thus, ACaR represents a new Ca^{2+} indicator that has

all the advantages of a ratiometric dye and is well suited for quantifying $[Ca^{2+}]$ in the cytoplasm and nucleoplasm of cardiac myocytes. The use of ratiometric imaging with ACaR yielded results almost identical to those obtained with the nonratiometric dye Fluo-4 (cf. Figs. 3 and 4), thus complementing and validating the calibration approach and the results obtained with Fluo-4.

The nuclear CaT consists of two components

Two important findings of this study are that the nuclear CaT exhibits distinct kinetics, and the nucleoplasmic systolic $[Ca^{2+}]$ peak consists of two components (one passive and one active). The passive component is most probably mediated by cytoplasmic Ca^{2+} diffusion through nuclear pore complexes to increase $[Ca^{2+}]_{nuc}$. Several lines of evidence support this notion. First, nuclear pore complexes are readily permeable to Ca^{2+} ions (7). Second, the nuclear CaT lags behind the cytoplasmic CaT (8). This delay is most likely caused by the time needed for diffusion of cytoplasmic Ca^{2+} through the nuclear pore complexes. In addition, the effective diffusion of Ca^{2+} within the nucleus is significantly slower than in the cytoplasm (35). Third, the amplitude of the nuclear CaT is proportional to the amplitude of the cytoplasmic CaT, providing further evidence for the passive nature of nuclear CaT (Fig. S2). On the other hand, some cells exhibited prominently higher nucleoplasmic diastolic $[Ca^{2+}]$ and higher nucleoplasmic systolic $[Ca^{2+}]$ peak. This implies that there is an additional source of Ca^{2+} in the nucleus. This observation is in line with previous findings that endothelin-1 can induce an independent increase in $[Ca^{2+}]_{nuc}$, without changing $[Ca^{2+}]_{cyto}$, and that this Ca^{2+} release originates from perinuclear stores (8). The exact mechanism by which cardiac myocytes can regulate their $[Ca^{2+}]_{nuc}$ independently from $[Ca^{2+}]_{cyto}$, and why some cells show prominently higher nucleoplasmic diastolic $[Ca^{2+}]$ than others remain to be determined. However, it is clear that the nucleus is a cellular compartment with its own perinuclear Ca^{2+} stores that is capable of actively storing and releasing Ca^{2+} (10). This supports the idea that nuclear envelope Ca^{2+} release plays an active role in nuclear Ca^{2+} signaling. It is believed that nuclear envelope Ca^{2+} release varies depending on the different physiological and pathophysiological processes taking place in the nucleus.

Perinuclear Ca^{2+} store content and Ca^{2+} leak determine the resting nucleoplasmic-to-cytoplasmic $[Ca^{2+}]$ gradient

Although investigations into the regulation of nuclear Ca^{2+} have been pursued for well over two decades by many laboratories using different technical approaches, there is still no consensus on the existence of resting $[Ca^{2+}]$ gradients between the nucleus and the cytoplasm. We consistently observed, after careful calibration with both Fluo-4 and

ACaR accounting for all the major technical problems with fluorescent indicators, a nucleoplasmic-to-cytoplasmic $[Ca^{2+}]$ gradient in all types of cardiac myocytes studied, and further sought to address the origin of the higher $[Ca^{2+}]_{nuc}$ during rest.

Both the nuclear envelope and the SR act as Ca^{2+} stores in cardiac myocytes (36). Furthermore, many lines of evidence suggest a direct connection of the nuclear envelope to the SR Ca^{2+} store. Because of the high mobility of Ca^{2+} inside this Ca^{2+} store (14), the luminal continuity of the entire nuclear envelope-SR store complex (14), and the existence of Ca^{2+} release channels in the nuclear envelope (37,38), Ca^{2+} can (in principle) be effectively mobilized from the nuclear envelope into the nucleoplasm. To test whether the nucleoplasmic-to-cytoplasmic $[Ca^{2+}]$ gradient is related to the Ca^{2+} load of the perinuclear Ca^{2+} stores, we applied CPA to deplete these stores. Depletion of Ca^{2+} led to a complete loss of the nucleoplasmic-to-cytoplasmic $[Ca^{2+}]$ gradient. This finding indicates that the Ca^{2+} load of the perinuclear stores is responsible for the nucleoplasmic-to-cytoplasmic $[Ca^{2+}]$ gradient, and suggests that a Ca^{2+} leak through nuclear envelope Ca^{2+} release channels facing the nucleoplasm causes the higher $[Ca^{2+}]$ in the nucleoplasm. A mismatch of SR Ca^{2+} pumps, which may be located primarily at the outer face of the nuclear envelope, could contribute to or even increase the nucleoplasmic-to-cytoplasmic $[Ca^{2+}]$ gradient (10).

Experiments with 2-APB and tetracaine clearly identified a 2-APB-sensitive Ca^{2+} leak pathway as the cause of the nucleoplasmic-to-cytoplasmic $[Ca^{2+}]$ gradient, suggesting that tonic Ca^{2+} release through perinuclear IP$_3$Rs is responsible for it. Furthermore, in electrically stimulated myocytes, 2-APB caused a selective decrease of nucleoplasmic $[Ca^{2+}]$ in diastole. These findings are in line with previous observations that perinuclear IP$_3$Rs are involved in regulation of $[Ca^{2+}]_{nuc}$ and excitation-transcription coupling (8,14,36,38). The results also provide further evidence for a segregation of Ca^{2+} release channels, suggesting that IP$_3$Rs are predominantly involved in nuclear Ca^{2+} regulation, whereas RyR2s are predominantly involved in cytoplasmic Ca^{2+} regulation in cardiomyocytes (37).

Stimulation frequency affects $[Ca^{2+}]_{nuc}$ and $[Ca^{2+}]_{cyto}$ differentially

Heart rate is an important determinant of cardiac function. In cardiac myocytes, stimulation frequency increases intracellular CaTs (39). This effect is largely caused by an increase in Ca^{2+} influx per unit time followed by an increased uptake of Ca^{2+} into the SR and subsequently an elevated SR Ca^{2+} load, which in turn increases the CaT. Because of the mostly passive nature of the nucleoplasmic CaT, which is governed largely by Ca^{2+} diffusion from the cytoplasm, one might assume that a similar frequency-dependent increase occurs in the nucleoplasmic CaT.

Indeed, systolic $[Ca^{2+}]_{nuc}$ increased in parallel with systolic $[Ca^{2+}]_{cyto}$ after an increase in stimulation frequency. Diastolic $[Ca^{2+}]_{nuc}$, on the other hand, increased with frequency to a much larger extent than diastolic $[Ca^{2+}]_{cyto}$. There was an ~8-fold increase in nucleoplasmic but only a ~4-fold increase in cytoplasmic diastolic $[Ca^{2+}]$ after an increase in stimulation frequency from 0.5 to 4 Hz. At 4 Hz stimulation, diastolic $[Ca^{2+}]$ reached ~800 nM in the nucleus but only ~400 nM in the cytoplasm. This large increase in diastolic $[Ca^{2+}]$ in the nucleus is due to the slow decay of the nucleoplasmic CaT, which is considerably slower than the cytoplasmic decay and thus leads to a much higher buildup of $[Ca^{2+}]_{nuc}$ when diastole is shortened. The results highlight the fact that a rather simple physiological maneuver, i.e., an increase in stimulation frequency, may lead to profound differences in the regulation of $[Ca^{2+}]_{nuc}$ versus $[Ca^{2+}]_{cyto}$, with important implications for frequency-dependent excitation-transcription coupling.

CONCLUSIONS

The approach presented here enables determination of $[Ca^{2+}]_{nuc}$ and quantification of Ca^{2+} fluxes between the cytoplasm and nucleus in cardiac myocytes, which is a prerequisite for elucidating the subcellular mechanisms involved in $[Ca^{2+}]_{nuc}$ regulation. In cardiac myocytes, $[Ca^{2+}]_{nuc}$ is a key determinant of excitation-transcription coupling (14,37). Our results show that 1), the nucleoplasmic CaT is composed of two components (one passive and one active); and 2), there is a substantial nucleoplasmic-to-cytoplasmic $[Ca^{2+}]$ gradient, particularly under resting conditions and in diastole. This gradient is dependent on intact intracellular Ca^{2+} stores, is mediated in part by Ca^{2+} leak/release through perinuclear IP$_3$Rs, and can be increased by increased stimulation frequencies. Altered $[Ca^{2+}]_{nuc}$ regulation, i.e., altered excitation-transcription coupling, may explain, at least in part, the altered expression of proteins in pacing-induced cardiomyopathies.

SUPPORTING MATERIAL

REFERENCES

1. Dibb, K. M., H. K. Graham, …, A. W. Trafford. 2007. Analysis of cellular calcium fluxes in cardiac muscle to understand calcium homeostasis in the heart. *Cell Calcium.* 42:503–512.

2. Eisner, D. A., H. S. Choi, …, A. W. Trafford. 2000. Integrative analysis of calcium cycling in cardiac muscle. *Circ. Res.* 87:1087–1094.

3. Bers, D. M. 2008. Calcium cycling and signaling in cardiac myocytes. *Annu. Rev. Physiol.* 70:23–49.

4. Zhang, S. J., M. Zou, …, H. Bading. 2009. Nuclear calcium signaling controls expression of a large gene pool: identification of a gene program for acquired neuroprotection induced by synaptic activity. *PLoS. Genet.* 5:e1000604.

5. Nicotera, P., and A. D. Rossi. 1994. Nuclear Ca^{2+}: physiological regulation and role in apoptosis. *Mol. Cell Biochem.* 135:89–98.

6. Sullivan, K. M., and K. L. Wilson. 1994. A new role for IP3 receptors: Ca^{2+} release during nuclear vesicle fusion. *Cell Calcium.* 16:314–321.

7. Stehno-Bittel, L., C. Perez-Terzic, and D. E. Clapham. 1995. Diffusion across the nuclear envelope inhibited by depletion of the nuclear Ca^{2+} store. *Science.* 270:1835–1838.

8. Kockskamper, J., L. Seidlmayer, …, B. Pieske. 2008. Endothelin-1 enhances nuclear Ca^{2+} transients in atrial myocytes through Ins(1,4,5)P3-dependent Ca^{2+} release from perinuclear Ca^{2+} stores. *J. Cell Sci.* 121:186–195.

9. Genka, C., H. Ishida, …, H. Nakazawa. 1999. Visualization of biphasic Ca^{2+} diffusion from cytosol to nucleus in contracting adult rat cardiac myocytes with an ultra-fast confocal imaging system. *Cell Calcium.* 25:199–208.

10. Gerasimenko, O., and J. Gerasimenko. 2004. New aspects of nuclear calcium signalling. *J. Cell Sci.* 117:3087–3094.

11. Bootman, M. D., D. Thomas, …, P. Lipp. 2000. Nuclear calcium signalling. *Cell Mol. Life Sci.* 57:371–378.

12. Echevarria, W., M. F. Leite, …, M. H. Nathanson. 2003. Regulation of calcium signals in the nucleus by a nucleoplasmic reticulum. *Nat. Cell Biol.* 5:440–446.

13. Badminton, M. N., A. K. Campbell, and C. M. Rembold. 1996. Differential regulation of nuclear and cytosolic Ca^{2+} in HeLa cells. *J. Biol. Chem.* 271:31210–31214.

14. Wu, X., T. Zhang, …, D. M. Bers. 2006. Local InsP3-dependent perinuclear Ca^{2+} signaling in cardiac myocyte excitation-transcription coupling. *J. Clin. Invest.* 116:675–682.

15. Zhang, T., and J. H. Brown. 2004. Role of Ca^{2+}/calmodulin-dependent protein kinase II in cardiac hypertrophy and heart failure. *Cardiovasc. Res.* 63:476–486.

16. Backs, J., and E. N. Olson. 2006. Control of cardiac growth by histone acetylation/deacetylation. *Circ. Res.* 98:15–24.

17. Little, G. H., A. Saw, …, C. Poizat. 2009. Critical role of nuclear calcium/calmodulin-dependent protein kinase IIdeltaB in cardiomyocyte survival in cardiomyopathy. *J. Biol. Chem.* 284:24857–24868.

18. Tucker, R. W., and F. S. Fay. 1990. Distribution of intracellular free calcium in quiescent BALB/c 3T3 cells stimulated by platelet-derived growth factor. *Eur. J. Cell Biol.* 51:120–127.

19. Bachs, O., N. Agell, and E. Carafoli. 1992. Calcium and calmodulin function in the cell nucleus. *Biochim. Biophys. Acta.* 1113:259–270.

20. Thomas, D., S. C. Tovey, …, P. Lipp. 2000. A comparison of fluorescent Ca^{2+} indicator properties and their use in measuring elementary and global Ca^{2+} signals. *Cell Calcium.* 28:213–223.

21. Connor, J. A. 1993. Intracellular calcium mobilization by inositol 1,4,5-trisphosphate: intracellular movements and compartmentalization. *Cell Calcium.* 14:185–200.

22. Perez-Terzic, C., L. Stehno-Bittel, and D. E. Clapham. 1997. Nucleoplasmic and cytoplasmic differences in the fluorescence properties of the calcium indicator Fluo-3. *Cell Calcium.* 21:275–282.

23. Gee, K. R., K. A. Brown, …, I. Johnson. 2000. Chemical and physiological characterization of fluo-4 Ca(2+)-indicator dyes. *Cell Calcium.* 27:97–106.

24. Giovannardi, S., and A. Peres. 1997. Nuclear and cytosolic calcium levels in NIH 3T3 fibroblasts. *Exp. Biol. Online.* 2:1–9.

25. McDonough, P. M., and D. C. Button. 1989. Measurement of cytoplasmic calcium concentration in cell suspensions: correction for

extracellular Fura-2 through use of Mn^{2+} and probenecid. *Cell Calcium.* 10:171–180.

26. Mitsui, M., A. Abe, M. Tajimi, and H. Karaki. 1993. Leakage of the fluorescent Ca^{2+} indicator fura-2 in smooth muscle. *Jpn. J. Pharmacol.* 61:165–170.

27. Kockskamper, J., K. A. Sheehan, …, L. A. Blatter. 2001. Activation and propagation of Ca(2+) release during excitation-contraction coupling in atrial myocytes. *Biophys. J.* 81:2590–2605.

28. Bers, D. M. 1982. A simple method for the accurate determination of free [Ca] in Ca-EGTA solutions. *Am. J. Physiol.* 242:C404–C408.

29. McGuigan, J. A., D. Luthi, and A. Buri. 1991. Calcium buffer solutions and how to make them: a do it yourself guide. *Can. J. Physiol Pharmacol.* 69:1733–1749.

30. Bers, D. M., C. W. Patton, and R. Nuccitelli. 1994. A practical guide to the preparation of Ca^{2+} buffers. *Methods Cell Biol.* 40:3–29.

31. Grynkiewicz, G., M. Poenie, and R. Y. Tsien. 1985. A new generation of Ca^{2+} indicators with greatly improved fluorescence properties. *J. Biol. Chem.* 260:3440–3450.

32. Maravall, M., Z. F. Mainen, B. L. Sabatini, and K. Svoboda. 2000. Estimating intracellular calcium concentrations and buffering without wavelength ratioing. *Biophys. J.* 78:2655–2667.

33. Nakajima, K., K. Harada, …, R. Shingai. 1993. Relationship between resting cytosolic Ca^{2+} and responses induced by N-methyl-D-aspartate in hippocampal neurons. *Brain Res.* 603:321–323.

34. Cannell, M. B., H. Cheng, and W. J. Lederer. 1994. Spatial non-uniformities in $[Ca^{2+}]i$ during excitation-contraction coupling in cardiac myocytes. *Biophys. J.* 67:1942–1956.

35. Soeller, C., M. D. Jacobs, …, M. B. Cannell. 2003. Application of two-photon flash photolysis to reveal intercellular communication and intracellular Ca^{2+} movements. *J. Biomed. Opt.* 8:418–427.

36. Kockskamper, J., A. V. Zima, …, . D. Bootman. 2008. Emerging roles of inositol 1,4,5-trisphosphate signaling in cardiac myocytes. *J. Mol. Cell Cardiol.* 45:128–147.

37. Bare, D. J., C. S. Kettlun, …, G. A. Mignery. 2005. Cardiac type 2 inositol 1,4,5-trisphosphate receptor: interaction and modulation by calcium/calmodulin-dependent protein kinase II. *J. Biol. Chem.* 280:15912–15920.

38. Zima, A. V., D. J. Bare, G. A. Mignery, and L. A. Blatter. 2007. IP3-dependent nuclear Ca^{2+} signalling in the mammalian heart. *J. Physiol.* 584:601–611.

39. Bers, D. M. 2001. Excitation-Contraction Coupling and Cardiac Contractile Force. Kluwer Academic Publishers, Dordrecht, The Netherlands.